communications physics

ARTICLE

https://doi.org/10.1038/s42005-023-01141-z OPEN

Noiseless single-photon isolator at room temperature

Shicheng Zhang [1,4], Yifan Zhan[1,4], Shangqing Gong[1,2,3] & Yueping Niu [1,2,3]✉

Nonreciprocal devices, such as isolators, are of great importance for optical communication and optical information processing. To bypass the limitation of a strong magnetic field imposed by the traditional Faraday magneto-optic effect, many alternative mechanisms have been proposed to demonstrate magnetic-free nonreciprocity. However, limited by the drive-induced noise, the noiseless isolator capable of working in the quantum regime has yet to be realized in the experiment. Here, we show a noiseless all-optical isolator with genuine single photons in hot atoms. We experimentally study this mechanism using an open V-type level scheme and demonstrate a low insertion loss of 0.6 dB and high isolation of 30.3 dB with bandwidth up to hundreds of megahertz. Furthermore, the nonreciprocal direction can be truly reversed only by tuning the frequency of the pump laser with the same setup. Our scheme relies on widely used optical technology and is thus universal and robust.

[1] School of Physics, East China University of Science and Technology, Shanghai 200237, China. [2] Shanghai Engineering Research Center of Hierarchical Nanomaterials, Shanghai 200237, China. [3] Shanghai Frontiers Science Center of Optogenetic Techniques for Cell Metabolism, Shanghai 200237, China. [4] These authors contributed equally: Shicheng Zhang, Yifan Zhan. ✉email: niuyp@ecust.edu.cn

Reciprocity, deriving from time-reversal symmetry, is a fundamental physical principle in the fields of electromagnetism, optics, and acoustics. In many practical applications, nonreciprocal devices, such as diodes in electronic circuits, are essential and powerful. In optics, the optical nonreciprocal devices, such as isolators, also play an irreplaceable role in both classical optical communications and quantum applications[1,2]. Optical nonreciprocity (ONR) is intrinsically difficult because of the time-reversal symmetry of light-matter interactions[3]. The traditional way of breaking the time-reversal symmetry of light is built on the magneto-optic effect[4]. It requires bulky magneto-optical materials and an external magnetic field and thus has limitations for on-chip or magnetic-sensitive quantum applications.

To bypass this limitation, considerable theoretical and experimental efforts have been made to explore the magnetic-free ONRs by using various physical mechanisms, including nonlinear effects[5–8], spatiotemporal modulation of permittivity[9–14], optomechanical interactions[15–18], moving Bragg lattices in atoms[19–21], chiral quantum systems[22–24], and random thermal-motion of atoms[25–31]. As we know, most of the reported schemes work in the classical region with weak coherent light. However, when it comes to quantum applications, where the information is encoded in individual photons, one basic requirement is that the ONR must be extended to genuine single photons. For single-photon isolators, it is not only required to have unidirectional transmittance but also more importantly, to maintain the quantum characteristics of input single photons from the selected direction. That is, the system should not introduce much additional noise, including the classical background noise[31] and quantum noise[32].

Many theoretical schemes have been proposed to realize single-photon ONRs[22,33–38]. Nonetheless, to date, only one experimental realization of an ONR with genuine single photons in ladder-type electromagnetically induced transparency[39] has been reported. To overcome the rapid dephasing of hot atoms, a strong drive field is necessary, which inevitably brings background noise photons to the signal due to nonlinear parametric processes. In addition, for such a coherent interaction, the amplitude and phase noise from the strong drive field will also induce nonnegligible quantum noise[40,41]. This deleterious noise induced by the strong drive field can damage the quantum characteristics of single photons. Recently, Hu et al. proposed a noiseless isolator via the incoherent population transfer process with a relatively low laser intensity, which can efficiently reduce the drive-induced noise[31]. However, they only demonstrated the quantum statistic properties of the scheme via the weak coherent laser and pseudothermal light source in their experiment. Until now, there has been no experimental demonstration of a noiseless ONR with genuine single photons, for the most part, because of the difficulty in filtering drive-induced background noise photons from extremely weak single-photon signals.

Here, we demonstrate a noiseless nonreciprocal proposal with genuine single photons based on incoherent optical pumping. Nonreciprocity is achieved utilizing velocity-selection-based incoherent population transfer. For hot atoms, when considering the Doppler effect, the optical pump process is dependent on the velocity of the atoms and the frequency of the pump field. If the pump field has proper detuning, it will induce an asymmetrical atomic population of the ground state which then leads to nonreciprocal absorption. Single-photon signals from one direction can pass through the atoms with negligible loss, while signals in the opposite direction will be absorbed. Due to the low intensity of the pump field and the great difference in frequency between the signal photons and the pump field, it is relatively easier to eliminate the pump-induced classical background noises in the experiment. More importantly, since the pump field only induces the incoherent population transfer, no quantum noise from the pump laser and atoms will be brought to the signal photons. In experiment, we demonstrate the noiseless properties by measuring the quantum-statistic conservation of the input genuine single photons and achieve an ultralow insertion loss of approximately 0.6 dB and high isolation of 30.3 dB with just a 40 mW pump field. Furthermore, the nonreciprocal bandwidth can be hundreds of megahertz, and the nonreciprocal direction can be reversed by simply reversing the detuning sign of the pump field.

Results and discussion

Basic principles. The mechanism and experimental setup of the optical isolator are shown in Fig. 1 which includes the single-photons generation system and ONR system. For the single-photons generation system, the photons are generated through the spontaneous four-wave mixing process[42]. In the presence of two counterpropagate coupling lasers, a pair of correlated photons (Stokes and Anti-Stokes) is generated in a paraffin-coated hot ^{87}Rb vapour cell, as shown in Fig. 1a. The relevant energy-level structure is shown in Fig. 1b. The generated photon pairs are collected by two opposing single-mode fibres with efficiencies of approximately 78% and 75%. The Stokes photons are detected by a single-photon counting module, and the heralded Anti-Stokes photons are collected to demonstrate the ONR in the forward and backward direction, as shown in Fig. 1c, and then detected by another single-photon counting module. For the ONR system, we use an open V-type atomic system consisting of a ground state $|5^2S_{1/2}, F=1\rangle(|1\rangle)$ and two excited states $|5^2P_{3/2}, F=2\rangle(|2\rangle)$ and $|5^2P_{1/2}, F=2\rangle(|3\rangle)$, see in Fig. 1d. A pump field, which propagates along $+x$ in the lab frame, couples the atomic transition of $|1\rangle$ and $|2\rangle$ with a detuning Δ_p. The Anti-Stokes photons, which propagate along the forward $(+x)$ or backward $(-x)$ direction, couple the atomic transition of $|1\rangle$ and $|3\rangle$ with a detuning Δ_s. For hot atoms, the random thermal-motion can create a Doppler shift. If an atom is moving toward or away from a laser source, it receives radiation that is blueshifted or redshifted. In the absence of the pump field, the forward- and backward-propagating signal photons are resonantly absorbed by the group of atoms with velocities $v=-\Delta_s/k$ and $v=\Delta_s/k$, respectively, where k is the wave vector and v is the atomic velocity. Since the velocity of atoms satisfies Maxwell's velocity distribution and is perfectly symmetrical, the population of the ground state is also symmetrical. Hence, the absorption of the atomic system is independent of the propagation direction of signal photons. That is, the atomic system is reciprocal to the signal photons. To achieve ONR, one needs to break the symmetry of the ground state population.

Then, we would like to understand what happens when a pump field propagates through the vapour cell. The pump field is applied to resonate with the transition of $|5^2S_{1/2}, F=1\rangle \rightarrow |5^2P_{3/2}, F=1\rangle$ and thus red detuned from the transition $|5^2S_{1/2}, F=1\rangle \rightarrow |5^2P_{3/2}, F=2\rangle$ by $\Delta_p = 2\pi \times 157$ MHz. It resonantly interacts with the group of atoms with a velocity of $v=-\Delta_p/k$ and leads to an incoherent population transfer from the ground state $|1\rangle$ to another metastable state $|5^2S_{1/2}, F=2\rangle$. However, for this group of atoms with a velocity of $v=\Delta_p/k$, the incoherent pumping effect is ignorable. Therefore, the population of the atoms with $v=-\Delta_p/k$ and $v=\Delta_p/k$ in the ground state becomes different. When $\Delta_s=\Delta_p$, for the forward signal photons, the population it 'feels' is empty, as shown in Fig. 1e. In contrast, the backward one 'feels' a full population. As a result, the forward signal photons can pass the atoms with ignorable absorption, while, the backward signal photons are strongly absorbed.

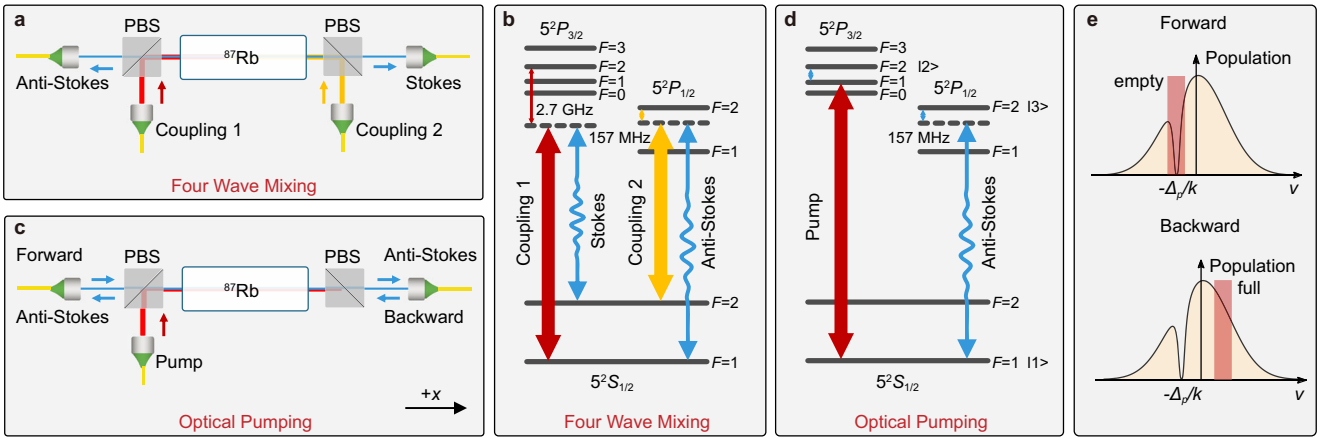

Fig. 1 Schematic diagram of the experimental setup and mechanism. a The heralded signal photons (Anti-Stokes) are generated through the four-wave mixing process in hot atoms. In the presence of two counter-propagating coupling laser beams, a pair of photons (Stokes and Anti-Stokes) are spontaneously generated and coupled into two opposed single-mode fibres. PBS: polarization beam splitter. **b** The Anti-Stokes photons are sent into an Rb cell for the demonstrating of single-photon optical nonreciprocity from the forward and backward direction, respectively. **c**, **d** represent the relevant atomic energy-level diagram for the four-wave mixing process and optical pumping process, respectively. Here, we use the Rb $5S \rightarrow 5P$ transition. F is the angular momentum quantum number. **e** The diagram of the ground state population versus the velocity of hot atoms. The optical pumping empties the ground state population of the group of atoms with a velocity of $v = -\Delta_p/k$, where Δ_p is the pump field detuning and k is the wave vector. Thus, the forward signal photons 'feels' empty population and the backward one 'feels' full empty, as shown in the shaded areas.

Optical pumping, in physics, is the use of light energy to elevate the atoms of the system from one energy level to another. The velocity selection of optical pumping has been used for the saturated absorption spectrum[43] and laser cooling[44]. Their objective is to overcome the Doppler-broadening limit by providing for a two-photon interaction that only occurs for atoms with a lab frame velocity very near zero. Although the basic principles are straightforward, we will only be able to unleash the full power of optical pumping by carefully attending to many details. In our scheme, the velocity-selection feature is used to break the symmetry of the ground state population and control the transmission of single photons. That is, the propagation direction of the signal photons is selected by the optical pumping process. The tremendous impact of the velocity-selective optical population effects suggests that our approach to ONR can be powerful as well. In addition, the nonreciprocal direction of our scheme is truly reversible, which can be achieved by simply tuning the frequency detuning of the pump field with the same frequency of the single photons.

Optical isolation. We first use a weak coherent probe field to scan the forward- and backward-propagation transmission spectra with varying pump field intensity, as shown in Fig. 2a. For the forward case, the transmission spectra show a high peak at a detuning of $\Delta_s = 2\pi \times 157$ MHz. As the intensity of the pump field increases, both the transmittance and bandwidth gradually increase. In contrast, the backward one always has nearly zero transmission. For the genuine single-photon experiment. We characterize the single-photon transmission by measuring the coincidence counts for the input Anti-Stokes photons, as shown in Fig. 2b. Additionally, we can see that as the pump field intensity increases the forward coincidence counts significantly increase. In contrast, the backward coincidence counts approach zero, revealing a strong single-photon ONR.

We define the single-photon transmission as $T_{f(b)} = CC_{f(b)}/CC_{in}$, with CC_{in} and $CC_{f(b)}$ representing the total integral coincidence counts for the initial input signal field and that after the forward (backward) propagation. Figure 3a shows the measured forward and backward single-photon transmissions as a function of the pump field Intensity. As the pump field intensity

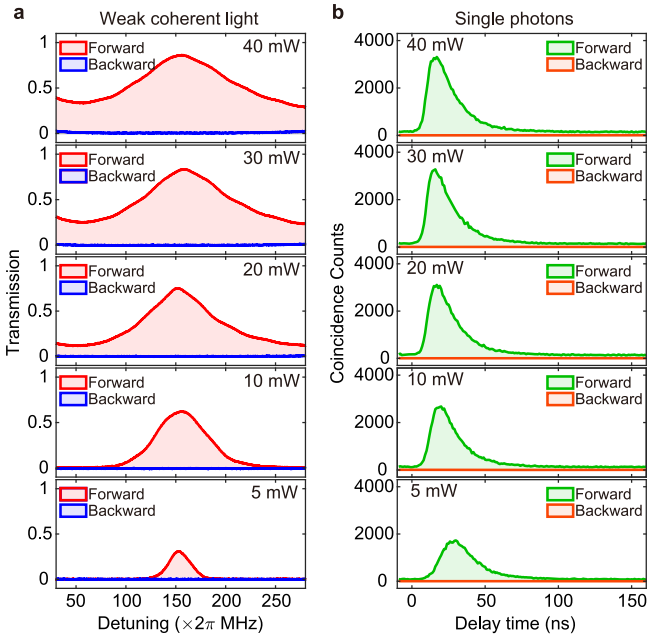

Fig. 2 Experimental observation of the non-reciprocity in hot atoms. **a** The forward (red) and backward (blue) propagation transmission spectra as a function of the weak probe field detuning Δ_s at the temperature of 80 °C. **b** The forward (green) and backward (brown) coincidence counts for 300 s as a function of the delay time τ with a temporal bin width of 1 ns.

increases from 5 mW to 40 mW, the forward-propagation transmission increases from 45.3% to 87.1%, whereas the backward-propagation transmission always vanishingly small. Under the condition of pump field intensity to 40 mW, we obtain an ultralow insertion loss of $-10\log(T_f) = 0.6$ dB and a strong isolation of $-10\log(T_b) = 30.3$ dB. For single-photon ONR, to obtain the best transmission, the bandwidth of the transmission peak should be much larger than the linewidth of the single photon itself. Figure 3b shows the measured bandwidth of the transmission peak for different pump field intensities. As the

intensity increases, the bandwidth increases from $2\pi \times 43$ MHz to $2\pi \times 175$ MHz.

Noise performance. The quantum characteristics of signal photons can be characterized by the second-order cross-correlation function $g^{(2)}_{a,as}(\tau)$. Figure 4a shows the measured $g^{(2)}_{a,as}(\tau)$ of the transmitted photons at a pump field intensity of 40 mW. The $g^{(2)}_{a,as}(\tau)$ of the input signal photons is shown in Fig. 4b. We can see that the maximum value of $g^{(2)}_{a,as}(\tau)$ for the forward signal photon is slightly larger than the input value. This is because the transmission spectra have limited bandwidth, and it can be seen as a narrowband filter that can filter the uncorrelated background photons. From the Fourier transform of $\sqrt{g^{(2)}_{a,as}(\tau) - 1}$[45], the calculated linewidth of the input single photons is approximately $2\pi \times 7.3$ MHz. We can see that the maximum bandwidth of the transmission peak is approximately 24 times the linewidth of the input single photons. Hence, it can ensure that the single-photon signal passes through the atomic medium. Expectedly, for the forward signal photon, its property is well preserved. In contrast, in the backward case, $g^{(2)}_{a,as}(\tau)$ is near 1, which means that the quantum characteristics is strongly broken. Moreover, we also measured the classical noise by blocking the signal while keeping the pump field on, see the blue line in Fig. 4b. The accidental coincidence from noise is measured to be below 0.1%.

To further evaluate the quantum characteristics of the single photons, we can use the heralded autocorrelation parameter α to benchmark the single-photon property[46]. When $\alpha < 0.5$, it indicates a near-single-photon character. In our experiment, the input single photons have $\alpha = 0.091 \pm 0.004$. After passing the nonreciprocal system in the forward direction, it becomes $\alpha = 0.093 \pm 0.007$. The result indicates perfect single-photon property preservation. In addition, we measure the Cauchy-Schwarz inequality R, which can be used to characterize the nonclassical correlation of the single photons. If $R > 1$, the photons are nonclassically correlated. In the absence of the nonreciprocal system, the measured parameter is 127. After the photons pass through the atomic system in the forward direction, we obtain $R = 129$. In contrast, we have $R = 0.27$ in the backward case, indicating the strongly broken nonclassical correlation. All the above results prove that our system does not introduce additional quantum noise.

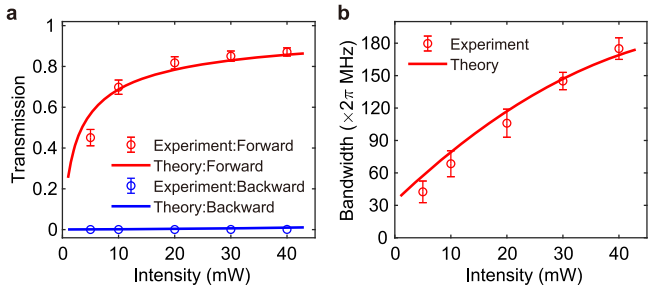

Fig. 3 Nonreciprocity performance versus the pump field intensity. a The measured forward (red) and backward (blue) transmission of heralded single photons after propagating through the atomic vapour versus the pump field intensity. **b** The measured bandwidth of the transmission peak as the function of the pump field intensity. The experimental data (circles) agree with the theoretical calculation (solid curves). The error bars are the standard deviation.

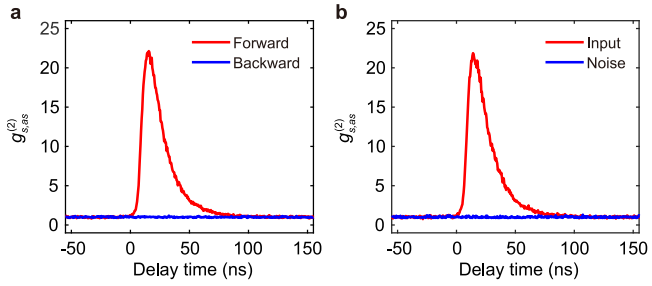

Fig. 4 Noise performance of the single-photon isolator. a The measured second-order cross-correlated function $g^{(2)}_{s,as}(\tau)$ of heralded single photons after propagating through the atomic vapour in the forward (red) and backward (blue) directions. **b** The measured second order cross-correlated function $g^{(2)}_{s,as}(\tau)$ of the input single photons (red) before the atomic vapour and the noise by blocking the signal while keeping the pump field on.

Reversed ONR. Reversible ONRs have important applications in reconfigurable nonreciprocal information processing. A practical reversible isolator needs to be able to work with the same input signals with the same performance index. In the work of Dong et al.[39], the nonreciprocal direction of the signals can be reversed by tuning the frequency of the control field. As reported, when the interaction varies from the electromagnetically induced transparency regime to the Raman regime, the frequency of the signal photons also needs to be tuned. In addition, the nonreciprocal bandwidth of the Raman process is almost the same order of magnitude as that of the single-photon signal generated from the atomic system. Thus, for genuine single photons, the isolation will be very poor. Thus, the reversible nonreciprocity may not be suitable for practical applications. In contrast, in our scheme, the nonreciprocal direction can be reversed by slightly tuning the frequency of the pump field but with the same frequency of the single photons. Figure 5 shows the measured forward and backward transmission with $\Delta_p = 157$ MHz (a) and $\Delta_p = -157$ MHz (b), respectively. Here, the pump field intensity is 40 mW and the temperature is 80 °C. For the two nonreciprocities, the frequency difference is just a few hundred megahertz and can be easily achieved using an acousto-optic modulator. Moreover, the two different nonreciprocal directions are based on the same physical mechanism, and they have the same transmission and isolation.

Conclusion

In summary, we have experimentally demonstrated a noiseless single-photon isolator at room temperature. We exploit an incoherent pumping-induced asymmetric ground state population to realize the ONR. Our approach is motivated by clear physical insights, and it is robust and easy to implement. A low insertion loss of approximately 0.6 dB and high isolation of 30.3 dB with a bandwidth of a few hundred megahertz are achieved in the experiment. Different from previous experiments,

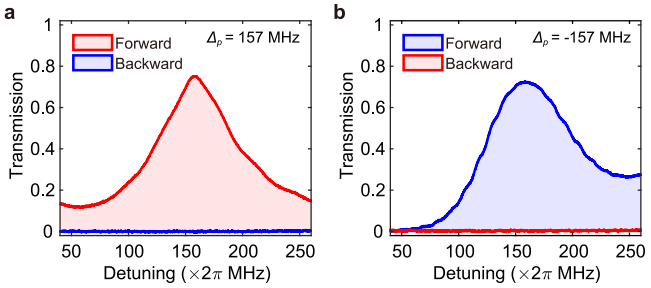

Fig. 5 Reversibility of the single-photon isolator. The forward (red) and backward (blue) propagation transmission spectra as a function of the weak probe field detuning with the detuning of the control field be $\Delta_p = 157$ MHz (**a**) and $\Delta_p = -157$ MHz (**b**), respectively.

our scheme can operate in the quantum regime without additional quantum noise. The quantum characteristics of the single photons can be well maintained in one direction, and be strongly broken in the opposite direction. The nonreciprocity is reconfigurable, and its direction can be reversed by simply tuning the frequency of the pump field without changing the frequency of the signal photons. The demonstration of a magnetic-free, noiseless, and reconfigurable single-photon isolator at room temperature may have potential applications in quantum networks and integrable quantum information processing since hot atoms can be miniaturized[47], integrated onto chips using one-dimensional waveguide structures[48], and mass-produced.

Methods

Experimental setup. For the four-wave mixing process, the two coupling lasers are supplied by two narrow-linewidth tunable diode lasers with wavelengths of 780 nm (Coupling 1) and 795 nm (Coupling 2). The coupling intensities are 10 mW and 40 mW, respectively. The two coupling fields have the same $1/e^2$ beam diameter of 2.4 mm. The coupling field 1 is red detuned by $2\pi \times 2.7$ GHz from the transition $|5^2S_{1/2}, F=1\rangle \rightarrow |5^2P_{3/2}, F=2\rangle$. The coupling field 2 is red detuned from the transition $|5^2S_{1/2}, F=2\rangle \rightarrow |5^2P_{1/2}, F=2\rangle$ by $2\pi \times 157$ MHz. The photon pairs are collected with a small angle of 0.5°. The Rb vapour cell has a length of 7.5 cm and is heated to 40 °C in the experiment. Before the Stokes photons enter the single-photon counting module (Excelitas SPCM-AQRH-16-APC), a 780 nm narrowband filter and a Fabry-Perot etalon (85% transmittance and 60 MHz bandwidth) are used to filter the stray coupling fields. The Anti-Stokes photons are focused by a lens with a focal length of 250 mm onto another ^{87}Rb vapour cell, which also has a length of 7.5 cm and is heated to 80 °C, for the demonstration of the ONR. The pump laser is supplied by another narrow-linewidth tunable diode laser with a wavelength of 780 nm. It is vertically polarized and can be reflected by the polarization beam splitter with an extinction ratio of approximately 35 dB. The Anti-Stokes photons are then collected by another single-mode fibre with an efficiency of 85%. To further filter the pump field, a 795 nm narrowband filter and another Fabry-Perot etalon (90% transmittance and 60 MHz bandwidth) are inserted before Anti-Stokes photons enter the single-photon counting module. This combination of polarization control, single-mode fibre, narrowband filter and Fabry-Perot etalon suppresses the pump field up to 120 dB, which makes the genuine single-photon experiment possible.

Characterization of the heralded single-photon. The second-order cross-correlation function of single photons is defined as $g^{(2)}_{s,as}(\tau) = \langle \hat{a}^\dagger_s(t)\hat{a}^\dagger_{as}(t+\tau)\hat{a}_{as}(t+\tau)\hat{a}_s(t)\rangle / [\langle \hat{a}^\dagger_s(t)\hat{a}_s(t)\rangle \langle \hat{a}^\dagger_{as}(t+\tau)\hat{a}_{as}(t+\tau)\rangle]$, where $\hat{a}^\dagger_s(t)(\hat{a}^\dagger_{as}(t+\tau))$ and $\hat{a}_s(t)(\hat{a}_{as}(t+\tau))$ denote the photon creation and annihilation operators for the Stokes (Anti-Stokes) photon at time $t(t+\tau)$. The heralded autocorrelation parameter α is defined as $\alpha = P_1P_{123}/P_{12}P_{13}$. We define that the generated Stokes photons are collected by the port 1. The Anti-Stokes photons passed through the nonreciprocal system are separated into two equal parts via a fiber beam splitter and then collected by the port 2 and 3. Thus, P_1 is the count of port 1, $P_{12}(P_{13})$ and is the twofold coincidence count between port 1 and 2(3), and P_{123} is the threefold coincidence count between the port 1, 2, and 3. The Cauchy-Schwarz inequality is defined as $R = [g^{(2)}_{s,as}(\tau)]^2 / g^{(2)}_{s,s}(0) g^{(2)}_{as,as}(0)$, with $g^{(2)}_{s,s}$ and $g^{(2)}_{as,as}$ being the auto-correlation functions of Stokes and Anti-Stokes photons, respectively.

Data availability

The data that support the plots within this paper and other findings of this study are available from the corresponding authors upon reasonable request.

Received: 3 August 2022; Accepted: 18 January 2023;
Published online: 07 February 2023

References

1. Gisin, N. & Thew, R. Quantum communication. *Nat. Photonics* **1**, 165–171 (2007).
2. Nielsen, M. A. & Chuang, I. L. *Quantum computation and quantum information* (Cambridge Univ. Press, 2011). https://doi.org/10.1017/CBO9780511976667.
3. Haus, H. A.*Waves and fields in optoelectronics* (Prentice-Hall, Englewood Cliffs, NJ, 1984).
4. Bi, L. et al. On-chip optical isolation in monolithically integrated non-reciprocal optical resonators. *Nat. Photonics* **5**, 758–762 (2011).
5. Fan, L. et al. An all-silicon passive optical diode. *Science* **335**, 447–450 (2012).
6. Chang, L. et al. Parity-time symmetry and variable optical isolation in active-passive-coupled microresonators. *Nat. Photonics* **8**, 524–529 (2014).
7. Bender, N. et al. Observation of asymmetric transport in structures with active nonlinearities. *Phys. Rev. Lett.* **110**, 234101 (2013).
8. Peng, B. et al. Parity-time-symmetric whispering-gallery microcavities. *Nat. Phys.* **10**, 394–398 (2014).
9. Guo, X., Ding, Y., Duan, Y. & Ni, X. Nonreciprocal metasurface with space-time phase modulation. *Light Sci. Appl.* **8**, 123 (2019).
10. Feng, L. et al. Nonreciprocal light propagation in a silicon photonic circuit. *Science* **333**, 729–733 (2011).
11. Yu, Z. & Fan, S. Complete optical isolation created by indirect interband photonic transitions. *Nat. Photonics* **3**, 91–94 (2009).
12. Lira, H., Yu, Z., Fan, S. & Lipson, M. Electrically driven nonreciprocity induced by interband photonic transition on a silicon chip. *Phys. Rev. Lett.* **109**, 033901 (2012).
13. Yu, Z. & Fan, S. Optical isolation based on nonreciprocal phase shift induced by interband photonic transitions. *Appl. Phys. Lett.* **94**, 171116 (2009).
14. Sounas, D. L. & Alù, A. Non-reciprocal photonics based on time modulation. *Nat. Photonics* **11**, 774–783 (2017).
15. Shen, Z. et al. Experimental realization of optomechanically induced non-reciprocity. *Nat. Photonics* **10**, 657–661 (2016).
16. Fang, K. et al. Generalized non-reciprocity in an optomechanical circuit via synthetic magnetism and reservoir engineering. *Nat. Phys.* **13**, 465–471 (2017).
17. Ruesink, F., Miri, M.-A., Alù, A. & Verhagen, E. Nonreciprocity and magnetic-free isolation based on optomechanical interactions. *Nat. Commun.* **7**, 13662 (2016).
18. Hafezi, M. & Rabl, P. Optomechanically induced nonreciprocity in microring resonators. *Opt. Express* **20**, 7672–7684 (2012).
19. Wang, D.-W. et al. Optical diode made from a moving photonic crystal. *Phys. Rev. Lett.* **110**, 093901 (2013).
20. Horsley, S. A. R., Wu, J.-H., Artoni, M. & La Rocca, G. C. Optical nonreciprocity of cold atom bragg mirrors in motion. *Phys. Rev. Lett.* **110**, 223602 (2013).
21. Ramezani, H., Jha, P. K., Wang, Y. & Zhang, X. Nonreciprocal localization of photons. *Phys. Rev. Lett.* **120**, 043901 (2018).
22. Xia, K. et al. Reversible nonmagnetic single-photon isolation using unbalanced quantum coupling. *Phys. Rev. A* **90**, 043802 (2014).
23. Sayrin, C. et al. Nanophotonic optical isolator controlled by the internal state of cold atoms. *Phys. Rev. X* **5**, 041036 (2015).
24. Scheucher, M., Hilico, A., Will, E., Volz, J. & Rauschenbeutel, A. Quantum optical circulator controlled by a single chirally coupled atom. *Science* **354**, 1577–1580 (2016).
25. Zhang, S. et al. Thermal-motion-induced non-reciprocal quantum optical system. *Nat. Photonics* **12**, 744–748 (2018).
26. Lin, G. et al. Nonreciprocal amplification with four-level hot atoms. *Phys. Rev. Lett.* **123**, 033902 (2019).
27. Hu, Y. et al. Multi-wavelength magnetic-free optical isolator by pumping in warm atoms. *Phys. Rev. Appl.* **12**, 054004 (2019).
28. Zhang, S. et al. Cavity-free circulator with low insertion loss using hot atoms. *Phys. Rev. Appl.* **14**, 024032 (2020).
29. Hu, Y. et al. Passive nonlinear optical isolators bypassing dynamic reciprocity. *Phys. Rev. Appl.* **16**, 014046 (2021).
30. Liang, C. et al. Collision-induced broadband optical nonreciprocity. *Phys. Rev. Lett.* **125**, 123901 (2020).
31. Hu, X.-X. et al. Noiseless photonic non-reciprocity via optically-induced magnetization. *Nat. Commun.* **12**, 2389 (2021).
32. Clerk, A. A., Devoret, M. H., Girvin, S. M., Marquardt, F. & Schoelkopf, R. J. Introduction to quantum noise, measurement, and amplification. *Rev. Mod. Phys.* **82**, 1155 (2010).
33. Tang, L. et al. On-chip chiral single-photon interface: Isolation and unidirectional emission. *Phys. Rev. A* **99**, 043833 (2019).
34. Wang, Z., Du, L., Li, Y. & Liu, Y.-X. Phase-controlled single-photon nonreciprocal transmission in a one-dimensional waveguide. *Phys. Rev. A* **100**, 053809 (2019).
35. Cheng, M.-T., Ma, X., Fan, J.-W., Xu, J. & Zhu, C. Controllable single-photon nonreciprocal propagation between two waveguides chirally coupled to a quantum emitter. *Opt. Lett.* **42**, 2914–2917 (2017).
36. Xu, X.-W., Chen, A.-X., Li, Y. & Liu, Y.-x Nonreciprocal single-photon frequency converter via multiple semi-infinite coupled-resonator waveguides. *Phys. Rev. A* **96**, 053853 (2017).
37. Ren, Y.-l et al. Nonreciprocal single-photon quantum router. *Phys. Rev. A* **105**, 013711 (2022).
38. Xu, X.-W., Chen, A.-X., Li, Y. & Liu, Y.-x Single-photon nonreciprocal transport in one-dimensional coupled-resonator waveguides. *Phys. Rev. A* **95**, 063808 (2017).

39. Dong, M.-X. et al. All-optical reversible single-photon isolation at room temperature. *Sci. Adv.* **7**, eabe8924 (2021).
40. Camparo, J. C. & Coffer, J. G. Conversion of laser phase noise to amplitude noise in a resonant atomic vapour: the role of laser linewidth. *Phys. Rev. A* **59**, 728 (1999).
41. Hsu, M. T. L. et al. Quantum study of information delay in electromagnetically induced transparency. *Phys. Rev. Lett.* **97**, 183601 (2006).
42. Zhu, L., Guo, X., Shu, C., Jeong, H. & Du, S. Bright narrowband biphoton generation from a hot rubidium atomic cell. *Appl. Phys. Lett.* **110**, 161101 (2017).
43. Bennett Jr, W. R. Hole burning effects in a He-Ne optical maser. *Phys. Rev.* **126**, 580 (1962).
44. Aspect, A., Arimondo, E., Kaiser, R., Vansteenkiste, N. & Cohen-Tannoudji, C. Laser cooling below the one-photon recoil energy by velocity-selective coherent population trapping. *Phys. Rev.* **61**, 826 (1988).
45. Thompson, J. K., Simon, J., Loh, H. & Vultetć, V. A High-brightness source of narrowband, identical-photon pairs. *Science* **313**, 74–77 (2006).
46. Grangier, P., Roger, G. & Aspect, A. Experimental evidence for a photon anticorrelation effect on a beam splitter: A new light on single-photon interferences. *Europhys. Lett.* **1**, 173 (1986).
47. Keaveney, J. et al. Cooperative lamb shift in an atomic vapor layer of nanometer thickness. *Phys. Rev. Lett.* **108**, 173601 (2012).
48. Sprague, M. R. et al. Broadband single-photon-level memory in a hollow-core photonic crystal fibre. *Nat. Photonics* **8**, 287–291 (2014).

Acknowledgements

We acknowledge the support of the National Natural Science Foundation of China (Grants No. 12004112, 12034007, and 11974109), Shanghai Natural Science Foundation (Grant No. 17ZR1442700) and Shanghai Sailing Program (Grant No. 20YF1410800). The work is also sponsored by "Chenguang Program" supported by Shanghai Education Development Foundation and Shanghai Municipal Education Commission (Grant No. 20CG35).

Author contributions

S.Z. and Y.N. contributed to the original idea, and supervised the experiment. S.Z. and Y.Z. built the experimental setup and carried out the measurements. They contributed equally to this work. S.G. supervised the whole project. All authors contributed to discussions of the results and writing of the manuscript.

Competing interests

The authors declare no competing interests.

Additional information

Correspondence and requests for materials should be addressed to Yueping Niu.

Peer review information *Communications Physics* thanks Jiangbin Gong, Alex Krasnok, and the other, anonymous, reviewer for their contribution to the peer review of this work.

Reprints and permission information is available at http://www.nature.com/reprints

Publisher's note Springer Nature remains neutral with regard to jurisdictional claims in published maps and institutional affiliations.

Open Access This article is licensed under a Creative Commons Attribution 4.0 International License, which permits use, sharing, adaptation, distribution and reproduction in any medium or format, as long as you give appropriate credit to the original author(s) and the source, provide a link to the Creative Commons license, and indicate if changes were made. The images or other third party material in this article are included in the article's Creative Commons license, unless indicated otherwise in a credit line to the material. If material is not included in the article's Creative Commons license and your intended use is not permitted by statutory regulation or exceeds the permitted use, you will need to obtain permission directly from the copyright holder. To view a copy of this license, visit http://creativecommons.org/licenses/by/4.0/.

© The Author(s) 2023, corrected publication 2023